Helical and Coil Conformations of Poly(ethylene glycol) in Isobutyric Acid and Water

Michael L. Alessi,[†] Alexander I. Norman,[†,‡] Sasha E. Knowlton,[‡] Derek L. Ho,[§] and Sandra C. Greer*[,†,‡]

Department of Chemical and Biomolecular Engineering and Department of Chemistry and Biochemistry, The University of Maryland College Park, College Park, Maryland 20742, and Center for Neutron Research, National Institute of Standards and Technology, Gaithersburg, Maryland 20899

Received June 23, 2005; Revised Manuscript Received August 19, 2005

ABSTRACT: We show that when poly(ethylene glycol) (PEG) is dissolved in isobutyric acid at temperatures below about 55 °C, the polymer molecule can form helices. Small-angle neutron scattering indicates that in pure isobutyric acid and in isobutyric acid-rich aqueous solutions the polymer chains form stiff rods that coexist with polymer coils when the polymer molecular weight is 2.38×10^4, 2.13×10^5, and 2.87×10^5 g/mol, but that at the lower molecular weight of 1.73×10^2, only the polymer rods form. The addition of chiral dopants causes a net optical rotation in the solution, indicating that the rods are actually helices. Above about 60 °C in deuterated isobutyric acid (and above about 70 °C in hydrogenated isobutyric acid), the helices convert to coils. In water, the PEG molecules form coils which persist over the entire temperature range studied (25−60 °C).

Introduction

Poly(ethylene glycol) (PEG) is a simple synthetic polymer: a chain of $[-O-CH_2-CH_2-]$ units, usually terminated on each end by an $-OH$ group. Other terminations are possible, e.g., $-OCH_3$, in which case the polymer is referred to as poly(ethylene oxide) (PEO). PEG has both hydrophobic segments (the carbon atoms) and hydrophilic segments (the oxygen atoms) and is soluble in both aqueous and organic solvents. The scientific literature on PEG is vast, amounting to about 90 000 articles. PEG has many practical applications, from detergents and paints to drug delivery and protein purification, and is arguably the most important water-soluble synthetic polymer.[1,2]

In the crystal,[3,4] the PEG unit cell is monoclinic, containing four chains. Each chain adopts a distorted structure with seven monomer units forming two helical turns. If the sequence $-O-CH_2-CH_2-O-$ has a gauche (g) conformation about the $-C-C-$ bond and a trans (t) conformation about the $-C-O-$ bond, then the conformation of the sequence is "ttg". The helical form of PEG consists of such ttg sequences. The reported X-ray diffraction data[3] show a wide distribution of the C−O torsional angles, suggesting that some C−O bonds are not at the minimum potential energy and implying a distorted helix. Scanning tunneling microscopy of PEO adsorbed on graphite shows single-, double-, and multistranded helices; the average width of the single helix is 7.6 Å.[4]

In water, the PEG molecule forms a loose coil.[5] There is some experimental evidence of short-range ttg sequences in PEG molecules in water,[6−9] but simulations show no such helical sequences.[10,11] The overall PEG conformation in water is that of a coil.

A study of the molecular weight distributions of polydisperse PEG in coexisting liquid phases has shown a remarkable fractionation of the PEG in a particular solvent system.[12] Water and isobutyric acid are mutually soluble above about 26 °C but separate into two liquid phases below the upper critical solution temperature at a mass fraction of about 39% isobutyric acid.[13,14] The molecular weight distributions of the PEG in the water-rich phase and in the isobutyric acid-rich phase were determined by size exclusion chromatography. It was found that the majority of the polymer mass was in the upper, isobutyric acid-rich phase. However, the majority of the higher molecular weight polymers were found to equilibrate into the lower, water-rich phase, and a significant reduction in polydispersity was observed in the water-rich phase. This observation led us to examine the conformations of the PEG in the coexisting phases.

We report here experimental evidence of a helical molecular conformation of PEG in this particular solvent, isobutyric acid. We study the PEG conformation in mixtures of water and isobutyric acid. In water-rich solutions, the PEG polymer chains form coils with the fractal dimension expected when excluded-volume interactions are present. In isobutyric acid-rich solutions, the polymer chains form stiff rods that coexist with coils at molecular weights of 2.38×10^4, 2.13×10^5, and 2.87×10^5, but only rods exist at the molecular weight of 1.73×10^2. At temperatures above about 60 °C in deuterated isobutyric acid (and above about 70 °C in hydrogenated isobutyric acid), the rods revert to coils.

We show, by using a chiral dopant to induce optical activity, that the rods are, in fact, helices. There are reports in the literature of polymers taking a helical form when chiral monomers are in the polymer backbone, or chiral side chains are attached to the polymer, or the polymer is in a chiral solvent.[15] Like the polyisocyanates in chloroform or hexane,[16] PEG in isobutyric acid is a polymer of achiral monomers in an achiral solvent, which takes a helical conformation. The PEG

[†] Department of Chemical and Biomolecular Engineering, The University of Maryland College Park.
[‡] Department of Chemistry and Biochemistry, The University of Maryland College Park.
[§] National Institute of Standards and Technology.
* Corresponding author. E-mail: sgreer@umd.edu.

10.1021/ma051339e CCC: $30.25
Published on Web 10/04/2005

Table 1. Commercial PEG Samples Used, Showing the Termination Groups, Lot Numbers, Weight Average Molecular Weight (M_w), Number Average Molecular Weight (M_n) and Polydispersity (M_w/M_n)

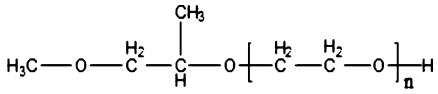

* end group =

PEG sample	lot no.	source	M_w g/mol	M_n g/mol	M_w/M_n
2kOH	PEG2OH-2K	Polymer Source	1.01×10^3	9.19×10^2	1.10
$2kOCH_3$	PEG2OCH3-2K	Polymer Source	1.73×10^3	1.56×10^3	1.11
8kOH	71K0114	Sigma	8.64×10^3	6.09×10^3	1.42
10kOH	PEG2OH-10K	Polymer Source	1.14×10^4	7.10×10^3	1.61
$10kOCH_3$	P2963-2OCH3	Polymer Source	1.29×10^4	5.84×10^3	2.21
20kOH	425182/1	Fluka	2.38×10^4	2.10×10^4	1.14
$200kOCH_3$	062725JO	Aldrich	1.51×10^5	7.29×10^4	2.08
252k*	P3624-EOOCH3	Polymer Source	2.87×10^5	2.48×10^5	1.16
$337kOCH_3$	P1590-EO	Polymer Source	2.13×10^5	1.53×10^5	1.40
$1000kOCH_3$	N/A	Polymer Source	9.33×10^6	4.57×10^6	2.04

helices occur as a racemic mixture, but an enantiomeric excess is induced by a chiral dopant.

Experimental Methods

Materials. Commercial PEG samples were used without further purification. The samples are listed in Table 1, where M_n is the number-average molecular weight, M_w is the weight-average molecular weight, and M_w/M_n is the polydispersity index. The molecular weights were all determined by size exclusion chromatography in our laboratory, as described below.

The solvents used were hydrogenated isobutyric acid (IBA, Aldrich Chemical Co., 99.9% purity), fully deuterated isobutyric acid (d-isobutyric acid or d-IBA, Isotec, Inc., 98% deuterated), D_2O (Isotec, Inc., 99.999% D), deuterated acetic acid (Aldrich, 99.9% D), DCl (Sigma-Aldrich, 99% D), and NaOD (Sigma-Aldrich, 99.9% D). Freshly distilled, deionized H_2O was obtained from a Nanopure system (Barnstead, 18 MΩ cm). The chiral dopants used in the polarimetry experiments were (*S*)-(+)-1,2-propanediol and (*R*)-(−)-1,2-propanediol (Lancaster Research Chemicals, 98% pure enantiomers).

The PEG concentrations studied by small-angle neutron scattering and by polarimetry were 12 ± 1 mg/mL, which are well below the estimated overlap concentrations for the above-listed PEG polymers in coil form. For PEG polymers in rod forms, the overlap concentrations are lower than for the coil forms[17] and approach 12 mg/mL or less for molecular weights greater than about 20 000.

Size Exclusion Chromatography (SEC). For the SEC analyses, all PEG samples were diluted to ∼2 mg/mL in freshly distilled, deionized water. Each sample was analyzed using an autosampler on a Waters SEC apparatus. The Waters SEC consists of a 1525 binary HPLC pump, a 2414 refractive index detector, a 2487 dual wavelength absorbance detector, and a 717 autosampler. A series of three Ultrahydrogel columns (120, 250, and 2000) of dimension 7.8 × 300 mm were placed in series in a column heater and set to 45 °C. A mobile phase of 0.01 M K_2HPO_4(aq) at pH = 7.065 was used. The apparatus was calibrated with known PEG standards (American Polymer Standards Corp., Mentor, OH) of molecular weight 2500, 10 225, 14 500, 30 225, 50 000, 111 000, 250 000, and 510 000 g mol^{-1}. Each sample was then injected for a run time of 60 min at a flow rate of 0.6 mL/min. An injection volume of 100 μL was used throughout. The subsequent chromatograms were analyzed and converted to full molecular weight distributions using the Waters software package Breeze, version 3.30.

Small-Angle Neutron Scattering (SANS). For the SANS measurements, the PEG was dissolved in d-isobutyric acid and D_2O, the deuteration of the solvent serving to reduce the incoherent background scattering and provide contrast with the hydrogenated polymer.

Small-angle neutron scattering (SANS) measurements were carried out using the NG7 30-m SANS instrument at the National Institute of Standards and Technology Center for Neutron Research (NCNR) in Gaithersburg, MD,[18] and were probed over the q range[19] from 0.0029 to 0.4014 $Å^{-1}$, where $q = (4\pi/\lambda)\sin(\theta/2)$, θ is the scattering angle, the wavelength λ is 8 Å, and $\Delta\lambda/\lambda$ is 0.11. Samples were loaded in either 1 or 2 mm path length quartz cells and closed with Teflon plugs. The raw data were corrected for background and parasitic scattering, placed on an absolute scale using a calibrated secondary standard, and circularly averaged to yield the scattered intensity $I(q)$. The incoherent background from the pure solvents was measured, corrected by the volume fraction displaced by the dissolved polymer, and subtracted from the reduced SANS data. The data points in the q range from ca. 0.3 to 0.4 $Å^{-1}$ were then averaged to yield the estimated incoherent background from polymer in the sample, which was subtracted from the data as well.

SANS data can be analyzed in three ways: (1) analyzing the slopes of $I(q)$ in various q ranges; (2) modeling of the data using specific models for the shapes and interactions of the scattering particles; (3) taking the Fourier transform of $I(q)$ into real space. In the analysis of the various q ranges of $I(q)$,[20] the Guinier regime at low q values ($qR_g \leq 1$, where R_g is the radius of gyration of the polymer chain) gives information about R_g:

$$\ln[I(q)] = \ln[I(0)] - \frac{q^2 R_g^2}{3} \quad (1)$$

where $I(0)$ is the scattering at $q = 0$. The fractal regime at intermediate q values gives information about particle shape; for example, the slope in the fractal regime is −1 for a rod and $-5/3$ for a coil with excluded volume. The Porod regime at high q values gives information about the interface between the particle and the solvent. The q value at which $I(q)$ changes from the Guinier regime to the fractal regime corresponds to $2\pi/L$, where L is the length of the particle. The transition from the fractal regime to the Porod downturn corresponds to $2\pi/D$, where D is the diameter of the particle.[21] However, the analysis of the q values at which $I(q)$ changes slope "can only be considered to be semi-quantitative, and ... does not usually provide accurate results."[22]

The second method of analysis is that using models, especially those provided by NCNR.[23] The analysis of SANS data for PEG solutions by Fourier transform (see below and Table 2, last column) indicated that under many conditions of molecular weight, solvent composition, and temperature the PEG molecules formed a mixture of coil and rod conformations. The presence of a mixture made the use of models problematic. In one case, (second sample in Table 2), the PEG formed only rodlike species, and in that case we applied the core−shell cylindrical model.[21] This model provides estimates of the cross-sectional radius and length of the core cylinder, assuming circular cross sections and monodisperse polymer chains. The volume fractions of the polymer and the scattering length densities of the solvents were fixed in that analysis.

Table 2. Values of Radius, R (Coil or Helix), Radius of Gyration, R_g (for a Coil, $R_g \approx R$), and D_{max} (See Text) for Various Molecular Weights of Linear PEG in Different Solvents at Different Temperatures[a]

mol wt, M_w g/mol	solvent	temp /°C	R/Å	R_g/Å	D_{max}/Å	helix or coil?
1.73×10^3	D_2O	60	12.0	16*	62	coil
1.73×10^3	dIBA/D_2O (0.39/0.61)	60	3.5 (3.3)		40 (34)	helix
1.73×10^3	AcOD	43	16.5	16.1*	75	coil
1.73×10^3	AcOD	55	16.5	17.5*	80	coil
2.38×10^4	D_2O	30	35.0	43*	185	coil
2.38×10^4	D_2O	55	41.3	46*	215	coil
2.38×10^4	D_2O	60	40	46*	190	coil
2.38×10^4	dIBA/D_2O (0.46/0.54)-2	30	6.0	43, 44*		coil + helix
2.38×10^4	dIBA/D_2O (0.46/0.54)-2	40	6.5	49, 60*		coil + helix
2.38×10^4	dIBA/D_2O (0.46/0.54)	45	5.5	57.6, 51*		coil + helix
2.38×10^4	dIBA/D_2O (0.46/0.54)	55	6.5	50.6, 49.2*		coil + helix
2.38×10^4	dIBA/D_2O (0.39/0.61)	60	3.5	28, 34.5*		coil + helix
2.38×10^4	dIBA	30	5.0	45, 42.4*		coil + helix
2.38×10^4	dIBA	43	5.0	41, 42.3*		coil + helix
2.38×10^4	dIBA	55	6.0	43.5, 38*		coil + helix
2.38×10^4	dIBA	60	40.0	46*	190	coil
2.38×10^4	AcOD	25	42.3	44*	250	coil
2.38×10^4	AcOD	55	44.0	45*	226	coil
2.38×10^4	AcOD/D_2O (0.39/0.61)	25	46.0	44*	200	coil
2.38×10^4	AcOD/D_2O (0.39/0.61)	55	46.0	42*	200	coil
2.38×10^4	DCl (0.1M)	25	39.4	42*	150	coil
2.38×10^4	DCl (0.001M)	25	41.0	40*	147	coil
2.38×10^4	NaOD (0.001M)	25	42.5	48*	195	coil
2.38×10^4	D_2O/NaCl	25	44.0	45*	195	coil
2.13×10^5	D_2O	60	130.0	200*	400	coil
2.13×10^5	dIBA/D_2O (0.46/0.54)-2	30	20.0 (3.3)	101*		aggregated helix
2.13×10^5	dIBA/D_2O (0.46/0.54)	55	50.0 (2.9)	77*		aggregated helix
2.13×10^5	dIBA	30	5	101		coil + helix
2.13×10^5	dIBA	43	6	120		coil + helix
2.13×10^5	dIBA	55	5.5	102		coil + helix
2.13×10^5	dIBA	60	130.0	161	320	coil
2.87×10^5	D_2O	43	87.0	90*	445	coil
2.87×10^5	D_2O	60	100.0	148*	300	coil
2.87×10^5	AcOD	43	56.0	62*	450	coil
2.87×10^5	AcOD	55	59.0	63*	450	coil
2.87×10^5	dIBA/D_2O (0.39/0.61)	43	16.0			aggregated helix
2.87×10^5	dIBA/D_2O (0.39/0.61)	55	24.0	71		aggregated helix + coil
2.87×10^5	dIBA	60	90.0	118*	234	coil

[a] Parameters are obtained from the $p(r)$ function, from Guinier plots (*), and from modeling to a core cylinder model (parentheses). The estimated uncertainties are ±0.6 Å for R and ± 5 Å for D_{max}, both from $p(r)$; ±1 Å for R_g from Guinier plots; ±0.1 Å for R from modeling. Abbreviations: dIBA = deuterated isobutyric acid; AcOD = deuterated acetic acid. Concentrations of solvents are given in mass fractions; "-2" means that the solvent was in two phases. The last column indicates the conformations of the PEG molecules. In mixtures of coil and helix, the R_g from $p(r)$ refers to the coils.

The third method of data analysis involves the Fourier transformation of the scattering data. The Fourier transformation of $I(q)$ involves the integral[24]

$$p(r) = \frac{1}{2\pi^2}\int_0^\infty I(q) qr \sin(qr)\, dq \qquad (2)$$

which yields the pair distance distribution function $p(r)$, where r is the distance in real space. The $p(r)$ is a histogram of the distances between pairs of points within the scattering object. The $p(r)$ can be calculated from SANS data using the generalized indirect Fourier transform (GIFT) method of Glatter and co-workers.[25] In our analysis, $p(r)$ data have been calculated using the GIFT software, PCG version 1.01.02.[26] The GIFT analysis used here assumes that the particles are so dilute as to be noninteracting, and thus it is not dependent on any model for the structure factor.

Thus, $p(r)$ provides additional information regarding the dimension, shape, and flexibility of the scattering species.[24,25,27−30] For example, spherical particles give rise to a symmetric $p(r)$ about a central maximum. A perfectly cylindrical particle will have a $p(r)$ with a very sharp peak at low values of r, which will then decrease (linearly if a rigid cylinder or approximately linearly with some oscillation if nonrigid) to a point where $p(r) = 0$. This $p(r) = 0$ point defines the longest distance in the scattering object, D_{max}, which is the same as the length, L, for a cylinder.

Polarimetry. If the PEG molecules form rods that are actually helices, then they will form left- and right-handed helices in equal number (a racemic mixture) and thus give no optical rotation. However, it is known that chiral impurities can lead to an "enantiomeric excess".[31−33] Therefore, we tested the effect of a chiral dopant on the optical rotation of the PEG in isobutyric acid to test for the presence of helices. The dopant was 1,2-propanediol, in either (+) or (−) enantiomer, at a mass fraction of 9×10^{-4}.

The Jasco P1010 polarimeter consists of a 10 cm path length glass cell with an interior volume of 8 mL. The P1010 uses a halogen lamp with a wavelength of 589 nm selected by a filter and has an accuracy of 0.002° with a reproducibility of 0.002° or better for measurements less than 1°. To measure the optical rotation, α, as a function of temperature, the polarimeter was configured with a VWR 1160 bath to circulate temperature-controlled water through a jacketed polarimeter cell (Jasco, 10 cm path length, 3.5 mL volume). Connecting Tygon tubing was insulated tightly with foam to minimize heat loss between the water bath and the sample. The temperature at the sample was measured with a thermistor connected to a Sper Scientific digital thermometer. The temperature was controlled and measured to an accuracy and precision of about 0.1 °C.

We first measured the optical rotation of solvent (hydrogenated isobutyric acid or H_2O) with added chiral dopant. We then dissolved PEG (12 mg/mL) into the solvent/dopant mixture and measured the optical rotation of that mixture. We subtracted the optical rotation of the solvent + dopant from the optical rotation of the solvent + dopant + PEG to obtain the optical rotation of the PEG. Each measurement was carried

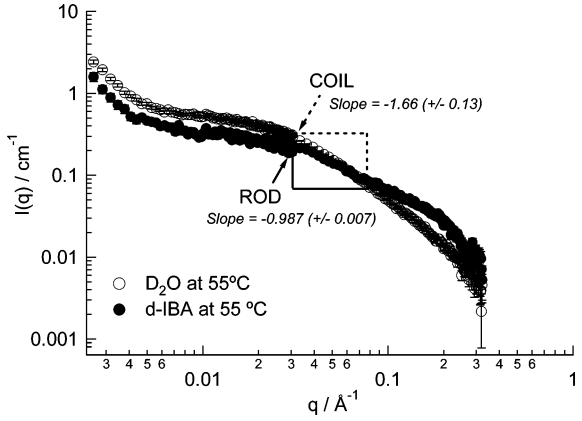

Figure 1. SANS intensity, I, as a function of wave vector, q, of PEG 20kOH ($M_w = 2.38 \times 10^4$), in D_2O and in d-isobutyric acid, at 55 °C. Slopes were calculated over the range $0.03 < q < 0.19$ Å^{-1} for the d-isobutyric acid solution and over the range $0.03 < q < 0.15$ Å^{-1} for the D_2O solution.

out by repeated integrations (10 s integration times) of the signal and corrected for concentration and background effects.

Results and Discussion

Uncertainties and error bars on graphs are given as one standard deviation.

Small-Angle Neutron Scattering (SANS). Measurements were made on PEG solutions with various solvent compositions and polymers of various molecular weights, at several temperatures. Plots of all the $I(q)$ data are available.[34] Table 2 gives the parameters from the SANS analysis.

For the system deuterated isobutyric acid + D_2O, the critical composition is 39% by mass of d-isobutyric acid and the critical temperature is about 42 °C,[35] so samples at this composition would be in the two-phase region for temperatures less than 42 °C; this condition did not occur for the 39% by mass samples. Samples with compositions that differ from 39% d-isobutyric acid will break into two liquid phases at temperatures less than 42 °C. Three samples that were in the two-phase region are indicated in Table 2 by "-2" on the solvent composition. For these samples, the SANS beam spanned the two phases and averaged over them.

Figure 1 shows a typical plot of $I(q)$ with the features typically seen in the SANS data for these systems. The data are for PEG 20kOH (see Table 1), $M_w = 2.38 \times 10^4$, in pure D_2O and in pure d-isobutyric acid at 55 °C. In D_2O, the slope at $q = 0.03-0.19$ Å^{-1} is close to $-5/3$, which is characteristic of a polymer coil with excluded volume.[20] In d-isobutyric acid, the slope at $q = 0.03-0.15$ Å^{-1} is close to -1, which is characteristic of a rod. The increase in SANS intensity at $q < 0.008$ Å^{-1} for both samples indicates that aggregates of polymer chains were also present, a well-known phenomenon in aqueous PEG solutions (see below). A high-q decrease in $I(q)$ occurs in d-isobutyric acid but not in D_2O; this is the Porod[36] regime with a slope of about -4, which indicates scattering from the sharp nonfractal interfaces of the rods, supporting the conclusion of a rod conformation in d-isobutyric acid and a coil conformation in D_2O.

In Figure 1 for polymer 20kOH in pure d-isobutyric acid, the transition points in $I(q)$ correspond to q values of about 0.030 Å^{-1} for $2\pi/L$ and about 0.20 Å^{-1} for $2\pi/d$. These would correspond to a rod of length $L \approx 209$ Å with a diameter $d \approx 31$ Å. Given the fact that the

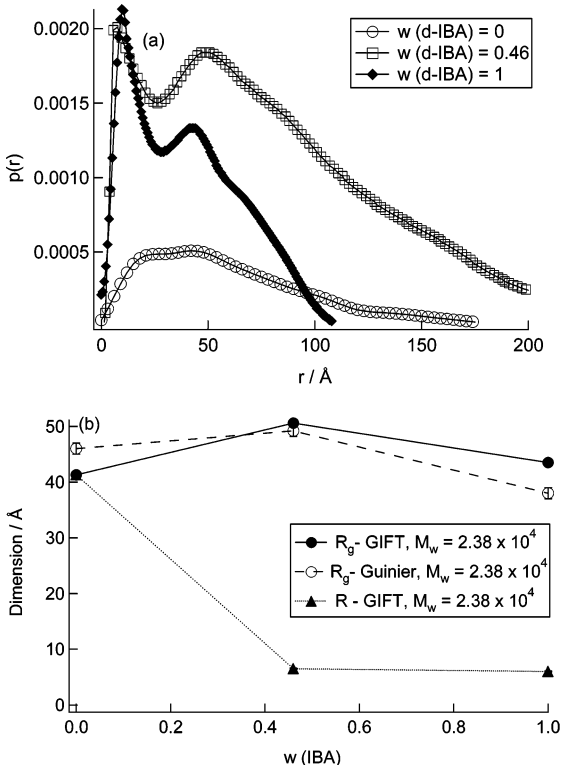

Figure 2. (a) The pair distance distribution function, $p(r)$, for PEG 20kOH, $M_w = 2.38 \times 10^4$, at 55 °C, for different mass fractions, w, of d-isobutyric acid in D_2O. (b) The radius of gyration (R_g) of PEG coils and the radius (R) of PEG rods (helices) for the system in (a), as obtained from GIFT analysis and Guinier plots, as a function of mass fraction of d-isobutyric acid in D_2O.

dimensions from the transition points are are subject to errors in determining the point of the slope change and are known not to be accurate,[22] we report only the values from model analyses, Guinier plots, and GIFT analyses in Table 2. Guinier plots were not possible for samples where the concentration exceeded the overlap concentration.

Solvent Concentration Dependence. Figure 2a shows $p(r)$ for the same data as Figure 1, for PEG 20kOH, $M_w = 2.38 \times 10^4$, at three compositions of d-isobutyric acid + D_2O. It is obvious that on changing solvent composition there is a dramatic change in the $p(r)$. The $p(r)$ for PEG in pure D_2O ($w = 0$) has one peak but is not symmetrical, indicating the PEG conformation to be an elongated coil, so that the maximum in $p(r)$ gives the radius of gyration, R_g, of 41.3 ± 1.2 Å, in agreement with the R_g determined from a Guinier plot (46.0 ± 0.6 Å). The coil shape is not spherical and has a maximum particle dimension of 215 Å.

The addition of d-isobutyric acid to a weight fraction of 0.46 brings about an overall increase in intensity and the appearance of a second peak at lower values of r. The inflection point of this intense, sharp peak yields the cross-sectional diameter of a rodlike particle.[25] The second, broader peak is due to the radius of gyration of coiled PEG. In other words, there is coexistence of coiled PEG and rodlike PEG under these conditions. The dimensions from $p(r)$ are $R_g = 50.6 \pm 1.2$ Å (cf. Guinier plot, 49.2 ± 0.6 Å) = radius of coil and $R = 6.5 \pm 0.1$ Å = radius of rod. The meaning of D_{max}, the point at which $p(r)$ goes to zero as r increases, becomes hard to interpret when both rods and coils are present and is, in fact, not well-determined by the GIFT procedure, so

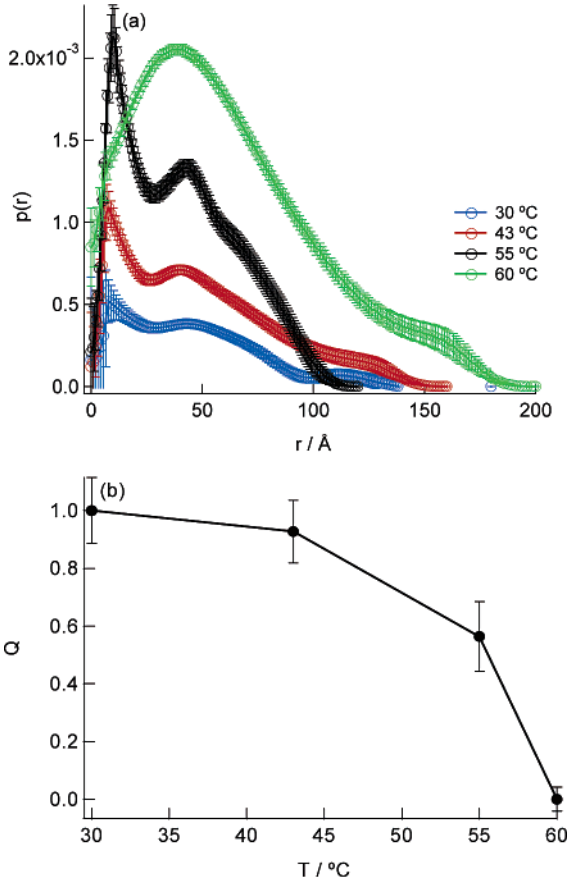

Figure 3. (a) Pair distance distribution function for PEG 20kOH, $M_w = 2.38 \times 10^4$, in pure d-isobutyric acid, for four different temperatures. (b) Relative invariant, Q, as a function of temperature for PEG 20kOH in pure d-isobutyric acid.

we do not list values of D_{max} except when only rods or only coils are present.

The differences between these two $p(r)$ profiles in Figure 2a are magnified when the solvent is pure d-isobutyric acid ($w = 1$). The peak corresponding to the cross section of a rod increases in intensity and resolution. The broad peak, corresponding to the radius of gyration of the coil, is reduced in intensity. Hence, the ratio of helical-to-coil conformations is increased with d-isobutyric acid content. Here R_g(coil) = 43.5 ± 1.2 Å (cf. Guinier plot, 38.0 ± 0.6 Å) and $R = 6.0 \pm 0.1$ Å.

Figure 2b plots the coil and rod radii as a function of mass fraction of d-isobutyric acid. The error bars indicate one standard deviation, so the dimensions from GIFT and Guinier analysis are in agreement, and there is no significant dependence of the dimensions on solvent composition.

Temperature Dependence. The $p(r)$ profiles for PEG 20kOH, $M_w = 2.38 \times 10^4$, in pure d-isobutyric acid at four different temperatures are given in Figure 3a. At low temperatures, a sharp peak is observed at low values of r, with a broad peak at higher values. As in Figure 2a, these peaks correspond to the cross-sectional diameter of a rod and the radius of gyration of a coil, respectively. The peak due to the coil increases in intensity (with respect to the rod peak) and resolution with temperature. This is evidence of a coexistence of coil and rod conformations of PEG in d-isobutyric acid that favors a rod at low temperatures and favors a random coil (forming an elongated spherical scattering particle) at temperatures of 60 °C and higher. R and R_g

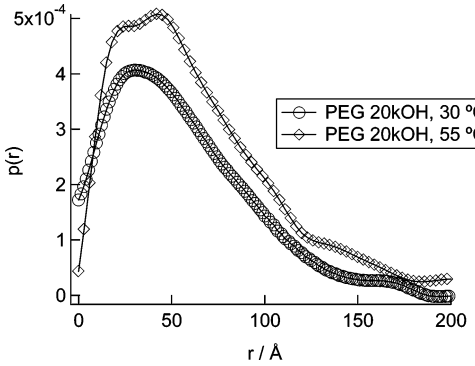

Figure 4. $P(r)$ for PEG 20kOH, $M_w = 2.38 \times 10^4$, in pure D_2O at 30 °C (open circles) and 55 °C (filled diamonds).

do not show any significant temperature dependence (see Table 2).

The relative invariant, Q, calculated from $Q = \int_{q_1}^{q_2} I(q)\, dq$ and normalized, is plotted in Figure 3b for PEG 20kOH in pure d-isobutyric acid. If we assume that helical rods scatter more than do random coils,[37] then the data in Figure 3b are consistent with this assumption, since Q decreases as the temperature increases. Figure 3b makes clear, from the gradual decrease in Q, that, in fact, coils and rods coexist at temperatures below 60 °C in pure d-isobutyric acid. Above 60 °C, only PEG coils exist.

The $p(r)$ for PEG 20kOH in pure D_2O at two temperatures are shown in Figure 4. The PEG has coil conformations at both temperatures. An elongated spherical scattering particle with $R_g \sim 45$ Å persists as the temperature is raised from 30 °C through to 55 °C. Clearly PEG forms coils in D_2O at all temperatures.

Molecular Weight Dependence. We have shown above that in pure d-isobutyric acid at temperatures above 60 °C the rod conformation of PEG 20kOH, $M_w = 2.38 \times 10^4$, changes to a coil conformation. Figure 5a shows $I(q)$ for PEG of a lower molecular weight, PEG 2kOCH$_3$ ($M_w = 1.73 \times 10^3$), in pure d-isobutyric acid at 60 °C. The core−shell cylinder model with $L = 40.0 \pm 1.2$ Å and $R = 3.3 \pm 0.1$ Å fits the SANS data very well. Figure 5b shows the $p(r)$ profile for this sample, which indicates a rigid rod with $L = 40.0 \pm 1.3$ Å and $R = 3.5 \pm 0.6$ Å. This is the smallest molecular weight that was studied and the only sample that indicated the presence of only rods/helices, even at 60 °C. This sample indicates that as the molecular weight of the polymer is reduced, the tendency for a helical structure is greater.

We note from Table 2 that R_g is larger in D_2O than in d-isobutyric acid at this temperature, indicating that D_2O is the better solvent for PEG. Figure 6 shows R_g of the polymer coils as obtained from $p(r)$ as a function of molecular weight in D_2O. The exponent of the molecular weight dependence is consistent (within error) with that expected (0.60) for a polymer coil in a good solvent.[38]

Polymer Aggregation. The formation of aggregates or clusters of PEG molecules in water has been well-known[39] but controversial, with arguments both that aggregation is the result of impurities[40−42] and that aggregation is an inherent property of PEG in water.[43−45]

In our SANS measurements, the aggregation of the PEG causes an increase in $I(q)$ at low q ($q < 0.003$ Å^{-1}). In the course of our studies, we observed samples with aggregation and samples without aggregation. All the polymer samples showed aggregation in D_2O and in mixtures of D_2O and d-isobutyric acid. In pure d-

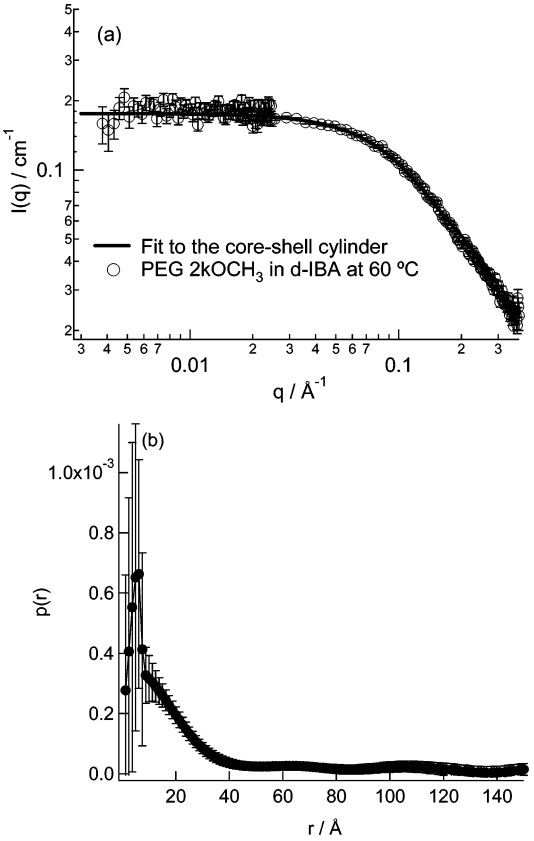

Figure 5. (a) SANS intensity profile for PEG 2kOCH$_3$ ($M_w = 1.73 \times 10^3$) in d-isobutyric acid + D_2O (0.39/61) at 60 °C and (b) the corresponding $p(r)$ profile.

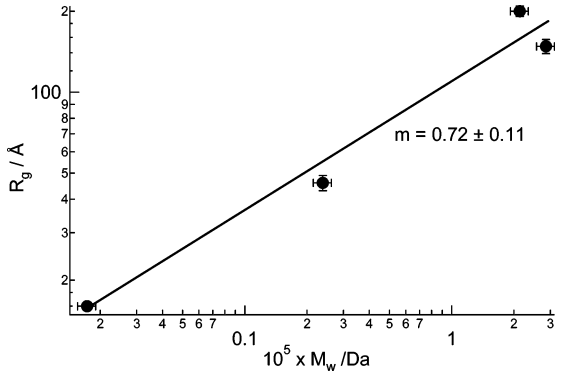

Figure 6. Radius of gyration, R_g, for PEG coils in D_2O as a function of weight-average molecular weight, at 60 °C.

isobutyric acid, the extent of aggregation depended on the molecular mass of the polymer: PEG of lower molecular mass showed less aggregation, such as PEG 2kOCH$_3$ as shown in Figure 5a. Thus, aggregation always occurred in the presence of D_2O, and aggregation occurred in d-isobutyric acid except at M_w less than or equal to 1.73×10^3.

Table 2 shows four samples at the highest molecular weights in which the values of R were considerably larger than those of the other samples. We interpret this as due to the aggregation of the helices into larger species.

Other Solvents. Our initial hypothesis was that the formation of the PEG rods was related to the pH of the solvent. We examined the SANS from PEG 20kOH in DCl (0.1 wt % in D_2O), in pure deuterated acetic acid and in NaOD (0.1 wt % in D_2O), all at 25 °C. In all three cases, the PEG assumed a coil conformation, indicating

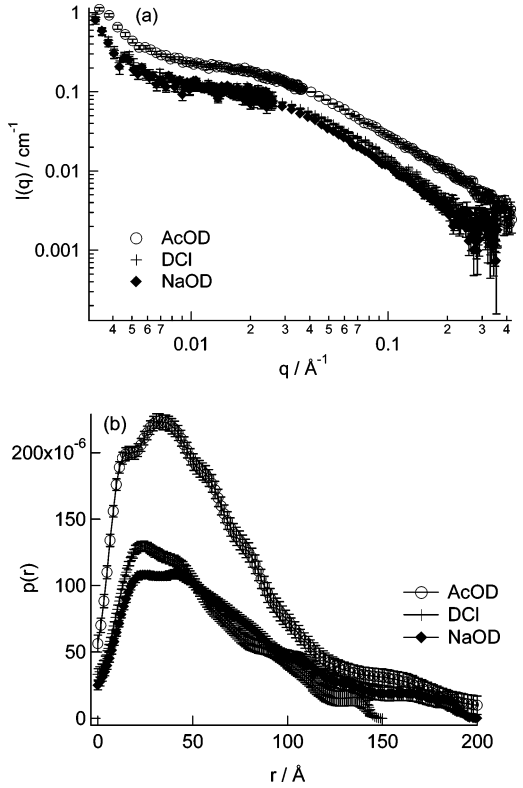

Figure 7. (a) SANS profiles for PEG 20kOH at 25 °C in different solvents: deuterated acetic acid, 0.1 wt % DCl in D_2O, and 0.1 wt % NaOD in D_2O. (b) The corresponding $p(r)$ profiles.

that the coil−rod transition in PEG is not a function of pH. Figure 7 shows $I(q)$ and $p(r)$ for these solvents. The $p(r)$ functions are typical of elongated spheres, corresponding to elongated polymer coils, for which dimensions are given in Table 2.

Polarimetry. PEG exhibited no optical rotation in H_2O containing a chiral dopant. PEG exhibited no optical rotation in (hydrogenated) isobutyric acid without a chiral dopant. However, PEG did indeed exhibit a net optical rotation in doped isobutyric acid. The observation of the induced optical rotation is evidence that the PEG "rods" seen by SANS are, in fact, helical in conformation. The optical rotation in doped isobutyric acid was larger, and the measurements were more reproducible when the sample was first heated above 60 °C and then cooled to room temperature. This is consistent with the observation from SANS that the PEG rod in d-isobutyric acid reverts to a coil at a temperature between 55 and 60 °C: Presumably the heating converts the helix to a coil, and the resulting coil is affected by the dopant when it refolds. All the samples on which we report here were first heated to 60 °C before the polarimetry measurements were made.

The first polarimetry studies were made at room temperature. Figure 8a shows that the sign of the optical rotation follows the chirality of the dopant: (+)-1,2-propanediol gives a (+) rotation for the PEG, and (−)-1,2-propanediol gives a (−) rotation for the PEG. Figure 8a also shows that the magnitude of the optical rotation of the PEG increases as the concentration of the dopant increases. Figure 8b shows the optical rotation as a function of the molecular weight of the PEG, for the PEG samples described above under "Experimental Methods, Materials". There is no clear dependence of the optical rotation on molecular weight, but there is a symmetry around 0° rotation in that the

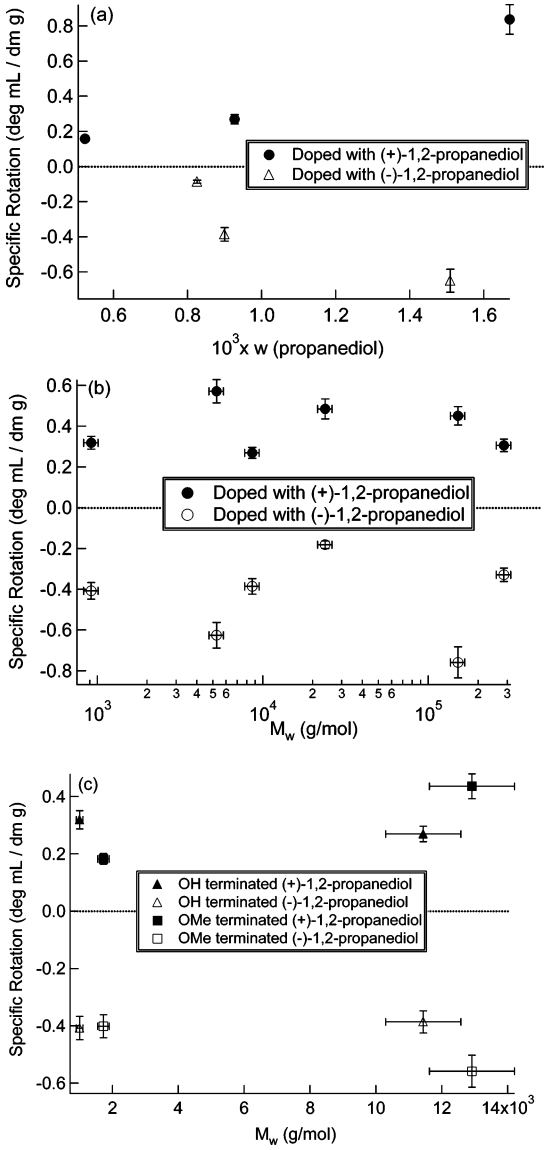

Figure 8. (a) Specific rotation of PEG 10kOH ($M_w = 1.14 \times 10^4$) in isobutyric acid with chiral dopants, (+)- and (−)-1,2-propanediol, as a function of mass fraction of dopant. (b) Specific rotation of PEG samples in isobutyric acid with chiral dopants, (+)- and (−)-1,2-propandiol at 0.1 mass %, as a function of PEG molecular weight. (c) Specific rotation of PEG samples in isobutyric acid with chiral dopants, (+)- and (−)-1,2-propanediol at 0.1 wt %, where the PEG has different polymer terminating groups. All these measurements were made at room temperature.

(−) and (+) dopants acted in equal and opposite directions on the induced PEG rotation, consistent with Figure 8a. Figure 8c shows the rotation of PEG samples with nearly the same molecular weights but with different terminating groups on the PEG molecules. There is no clear pattern of end effects.

Next we measured the optical rotation of PEG in doped isobutyric acid as a function of temperature. Figure 9 shows the magnitude of the optical rotation as a function of temperature for 20kOH PEG doped in both (+)- and (−)-1,2-propanediol enantiomers. For each measurement, the sample was allowed to reach equilibrium (∼15 min) before the next measurement was taken. For both enantiomers, the induced optical rotation decreases as the temperature increases and becomes zero at about 70 °C. We propose that the disappearance of the optical rotation indicates the

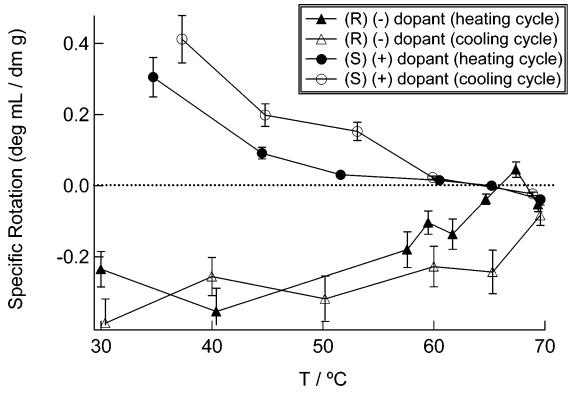

Figure 9. Specific rotation of PEG 20kOH ($M_w = 2.38 \times 10^4$) in hydrogenated isobutyric acid with chiral dopants, (+)- and (−)-1,2-propanediol, as a function of temperature.

unfolding of the PEG helices into coils. This result in hydrogenated isobutyric acid is to be compared with the SANS results (see Figure 3) in deuterated isobutyric acid that show a helix−coil transition at 60 °C. That the optical rotation does not change abruptly indicates that the helix-to-coil transition occurs slowly over a temperature range and that a coexistence of helices and coil conformations persists, consistent with the observations made by SANS (Figure 3). When the samples are cooled, the optical rotation reappears, indicating the conversion of the coils back to helices.

We observe the helix−coil transition at about 60 °C in deuterated isobutyric acid and at about 68 °C in hydrogenated isobutyric acid. This suggests that the helix is more stable in hydrogenated isobutyric acid than in deuterated isobutyric acid. We do not understand this difference.

Summary and Conclusions

We find that in isobutyric acid PEG molecules can take the form of helices at temperatures below about 68 °C. There is a coexistence of helices and coils for higher molecular weights, but at low molecular weight the polymers form only helices. The PEG helices revert to coils above about 68 °C in hydrogenated isobutyric acid (and above about about 60 °C in deuterated isobutyric acid). We know of no other solvent in which PEG has the helical conformation. We confirm that PEG molecules form coils in D_2O.

The coexistence of PEG coils and PEG helices can have two forms: Each PEG molecule can form either a coil or a helix, or each PEG molecule can itself be part coil and part helix. It is difficult to distinguish between the two from the neutron scattering data. We would expect $p(r)$ to have a more complex form in the case of polymers that are mixed coils and helices, and thus we tend to favor the case of polymers as either coils or helices, but we cannot firmly prove that at this time.

Why do the PEG molecules form helices in isobutyric acid? We can imagine three mechanisms: (1) there is a steric effect of the isobutyric acid with the PEG that induces the helical conformation; (2) the water present as a hydration layer on the PEG (even in pure isobutyric acid) serves as a solvophilic layer and the PEG forms a helix to best present that layer to the solvent; (3) the water present in the hydration layer is released by the formation of the helix, thus increasing the entropy and driving the conformational change. We are designing new experiments to test these mechanisms.

Our study was initially motivated by an effort to understand the microscopic origins of the dramatic fractionation of PEG in a solution of water + isobutyric acid.[12] Water and isobutyric acid are mutually soluble above about 26 °C but separate into two liquid phases below the upper critical solution temperature (UCST).[13,14] When PEG is added to the two-phase water + isobutyric acid system, the longer polymer chains tend to go to the lower, aqueous phase and the shorter polymer chains tend to go to the upper, acidic phase. The average molecular weight in the lower phase is about twice that in the upper phase. The greater mass of the polymer (~80%) is in the upper, acidic phase, even though PEG is more soluble in water than in isobutyric acid.[12] This new work has shown that the PEG molecules are coils in the water phase and helices in the isobutyric acid phase. We hope that the elucidation of the mechanism of the helix formation will elucidate the fractionation behavior as well.

Acknowledgment. This research was supported by the National Science Foundation, Chemistry Division. We also acknowledge support of the National Institute of Standards and Technology (NIST), U.S. Department of Commerce, in providing the neutron research facilities used in this work. We thank Jack Douglas, Philip R. Deshong, Lyle Isaacs, Yiwei Fei, and Andrew Lyon for helpful discussions. Certain products and equipment are mentioned by name only to clarify the experimental conditions used; this does not mean that they are the best for the purpose or that NIST endorses them.

References and Notes

(1) Bailey, F. E.; Koleske, J. V. *Alkylene Oxides and Their Polymers*; Marcel Dekker: New York, 1991; Vol. 35.
(2) Harris, J. M., Zalipsky, S., Eds. *Poly(ethylene glycol): Chemistry and Biological Applications*; American Chemical Society: Washington, DC, 1997; Vol. 680.
(3) Takahashi, Y.; Tadokoro, H. *Macromolecules* **1973**, *6*, 672−675.
(4) Yang, R.; Yang, X. R.; Evans, D. F.; Hendrikson, W. A.; Baker, J. *J. Phys. Chem.* **1990**, *94*, 6123−6125.
(5) Vennaman, N.; Lechner, M. D.; Oberthuer, R. C. *Polymer* **1987**, *28*, 1738−1748.
(6) Matsuura, H.; Fukuhara, K. *J. Mol. Struct.* **1985**, *126*, 251−260.
(7) Yang, X.; Su, Z.; Wu, D.; Hsu, S. L.; Stidham, H. D. *Macromolecules* **1997**, *30*, 3796−3802.
(8) Begun, R.; Matsuura, H. *J. Chem. Soc., Faraday Trans.* **1997**, *93*, 3839−3848.
(9) Oesterhelt, F.; Rief, M.; Gaub, H. E. *New J. Phys.* **1999**, *1*, 6.1−6.11.
(10) Smith, G. D.; Bedrov, D.; Borodin, O. *J. Am. Chem. Soc.* **2000**, *122*, 9548−9549.
(11) Bedrov, D.; Smith, G. D. *J. Chem. Phys.* **2003**, *118*, 6656−6663.
(12) Shresh, R. S.; MacDonald, R. C.; Greer, S. C. *J. Chem. Phys.* **2002**, *117*, 9037−9049.
(13) Greer, S. C. *Phys. Rev. A* **1976**, *14*, 1770−1780.
(14) Venkataraman, T. S.; Narducci, L. M. *J. Phys. C: Solid State Phys.* **1977**, *10*, 2849−2861.
(15) Green, M. M.; Park, J.-W.; Sato, T.; Teramoto, A.; Lifson, S.; Selinger, R. L. B.; Selinger, J. V. *Angew. Chem., Int. Ed.* **1999**, *38*, 3138−3154.
(16) Lifson, S.; Andreola, C.; Peterson, N. C.; Green, M. M. *J. Am. Chem. Soc.* **1989**, *111*, 8850−8858.
(17) Teraoka, I. *Polymer Solutions: An Introduction to Physical Properties*; Wiley-Interscience: New York, 2002.
(18) Glinka, C. J.; Barker, J. G.; Hammouda, B.; Krueger, S.; Moyer, J. J.; Orts, W. J. *J. Appl. Crystallogr.* **1998**, *34*, 430−445.
(19) *NG3 and NG7 30-Meter SANS Instruments Data Acquisition Manual*; Cold Neutron Research Facility at the National Institute of Standards and Technology, 2002.
(20) Higgins, J. S.; Benoit, H. C. *Polymers and Neutron Scattering*; Clarendon Press: Oxford, 1994.
(21) Schurtenberger, P. In *Neutrons, X-rays, and Light Scattering Methods Applied to Soft Condensed Matter*; Lindner, P., Zemb, T., Eds.; Elsevier Science B.V.: New York, 2002; p 541.
(22) Pedersen, J. S.; Schurtenberger, P. *Macromolecules* **1996**, *29*, 7602−7612.
(23) http://www.ncnr.gov/resources/index.html.
(24) Glatter, O. In *Neutrons, X-rays, and Light: Scattering Methods Applied to Soft Condensed Matter*; Lindner, P., Zemb, T., Eds.; Elsevier: Amsterdam, 2002; p 73.
(25) Glatter, O. In *Neutron, X-ray, and Light Scattering: Introduction to an Investigative Tool for Colloidal and Polymeric Systems*; Lindner, P., Zemb, T., Eds.; North-Holland: New York, 1990; pp 33−82.
(26) GIFT software available from O. Glatter, U. o. G., Austria. Details can be found at the Web site http://physchem.kfunigraz.ac.at/sm/.
(27) Glatter, O. *J. Appl. Crystallogr.* **1977**, *10*, 415−421.
(28) Glatter, O. *J. Appl. Crystallogr.* **1980**, *13*, 577−584.
(29) Glatter, O. In *Neutrons, X-rays, and Light: Scattering Methods Applied to Soft Condensed Matter*; Lindner, P., Zemb, T., Eds.; Elsevier: Amsterdam, 2002; p 103.
(30) Hansen, S. *J. Appl. Crystallogr.* **2003**, *36*, 1190−1196.
(31) Soai, K.; Shibata, T.; Sato, I. *Acc. Chem. Res.* **2000**, *33*, 382−390.
(32) Singleton, D. L.; Vo, L. K. *J. Am. Chem. Soc.* **2002**, *124*, 10010−10011.
(33) Yashima, E. *Anal. Sci.* **2002**, *18*, 3−6.
(34) Alessi, M. L. Ph.D. Dissertation; University of Maryland: College Park, MD, 2004; p 162.
(35) Greer, S. C. *Ber. Bunsen-Ges. Phys. Chem.* **1977**, *81*, 1079−1081.
(36) Porod, G. *Kolloid-Z.* **1951**, *124*, 83−114.
(37) Koh, A. Y. C.; Heenan, R. K.; Saunders, B. R. *Phys. Chem. Chem. Phys.* **2003**, *5*, 2417−2423.
(38) Grosberg, A. Y.; Khokhlov, A. R. *Statistical Physics of Macromolecules*; American Institute of Physics: New York, 1994.
(39) Polverari, M.; van de Ven, T. G. M. *J. Phys. Chem.* **1996**, *100*, 13687−13695.
(40) Devanand, K.; Selser, J. C. *Nature (London)* **1990**, *343*, 739−741.
(41) Porsch, B.; Sundelof, L.-O. *Macromolecules* **1995**, *28*, 7165−7170.
(42) Faraone, A.; Magazu, S.; Maisano, G.; Migliardo, P.; Tettamanti, E.; Villari, V. *J. Chem. Phys.* **1999**, *110*, 1801−1806.
(43) Hammouda, B.; Ho, D.; Kline, S. *Macromolecules* **2002**, *35*, 8578−8585.
(44) Ho, D. L.; Hammouda, B.; Kline, S. R. *J. Polym. Sci., Part B: Polym. Phys.* **2003**, *41*, 135−138.
(45) Duval, M. *Macromolecules* **2000**, *33*, 7862−7867.

MA051339E